2nd International Conference on Electrical Engineering Applications (ICEEA'2025), Ahmadu Bello University, Zaria, Nigeria, November 10-12, 2025.

Analysis of the Effect of Inductance and Rotor Position on the Performance of a Switched Reluctance Motor Using Geometry-Based Analytical Method

Ameh Onoja
Department of Electrical & Electronics Engineering, Federal University of Technology, Minna, Nigeria
onoja.pg202320700@st.futminna.edu.ng

Enesi Asizehi Yahaya
Department of Electrical & Electronics Engineering, Federal University of Technology, Minna, Nigeria.
enesi.asizehi@futminna.edu.ng

Jacob Tsado
Department of Electrical & Electronic Engineering. Federal University of Technology, Minna, Nigeria.
tsadojacob@futminna.edu.ng

***Abstract*— This paper investigates the impact of inductance and rotor position on the performance of a 4-phase, 8/6 Switched Reluctance Motor (SRM) in electric drive systems. The study employs a geometry-based analytical model using Ansys-Maxwell software to investigate the inductance profile, which aids in identifying key torque regions, ensuring sound design and control optimisation. To study the performance characteristics of a switched reluctance motor, the relationship between inductance and rotor position is vital, as it directly influences torque generation, efficiency, and dynamic response. The model provides a computationally efficient foundation for performance assessment and future enhancements using numerical methods. The results obtained show that while the inductance variation relative to rotor position drives torque production, saturation at high currents limits motor performance, therefore, the phase current need to be properly managed to ensure optimal performance.**

Keywords— Switched reluctance motor, Inductance and Rotor Position, Geometry-Based analytical method (GBAM), inductance, rotor position

I. Introduction

Modern electric drive applications are increasingly adopting switched reluctance motors (SRMs) due to their cost-effectiveness, robustness, and simple construction [1]. A switched reluctance motor (SRM) is characterised by its doubly salient design, featuring no rotor windings and tightly arranged excitation windings on the stators [2][3]. The system operates on the principle of variable reluctance, generated by the sequential excitation of the stator phases through an electronic controller [4][5]. The torque produced is significantly influenced by the rotor position and stator current, due to the non-linear and highly saturated magnetic characteristics of the switched reluctance motor during rotor transitions [6][7].

This paper explores the significance of phase inductance variation with rotor position, analysing its effect on motor performance. An analytical assessment based on geometry using Ansys-Maxwell software is conducted to investigate the influence of inductance and rotor position on an 8/6 switched reluctance motor. Although the analytical method provides a quick estimate of motor inductance, it is limited by the simplicity of the magnetic circuit and the requirement for accurate geometry and material data, which can be challenging to obtain. The inductance profile and rotor position of a switched reluctance motor are essential characteristics that influence the motor's overall performance [5]. This profile is established by analysing the relationship between inductance and rotor position at three points: the aligned, unaligned, and intermediate positions [8].

Various methods for determining the inductance profile of the switched reluctance motor (SRM) have been explored; however, these techniques require complicated computational processes, relying on data from finite element analysis (FEA) models or experimental setups [9]. Current analytical models frequently overlook the nonlinear characteristics of magnetic materials, especially the impact of saturation at elevated currents, which can substantially influence inductance and torque production [2][10].

This paper investigates the effect of inductance and rotor position on the performance of an 8/6 switched reluctance motor employing the geometry-based analytical model using the Ansys-Maxwell software

II. Methodology

Analytical models greatly assist in machine analysis and are very useful during the initial design stage, as they are computationally efficient. These methods leverage the geometric parameters to predict and optimise the motor's performance. This paper investigates the effect of inductance and rotor position on the performance of a switched reluctance motor using the Geometry-Based Analytical Method (GBAM).

According to [9], a geometry-based analytical method, GBAM, is developed as follows:

Calculation of aligned inductance:

The inductance of a magnetic circuit is expressed as:

$$L = \frac{N^2}{\mathcal{R}} \quad (1)$$

Where N is the number of turns per pole and $\mathcal{R}$, is the sum of the reluctance around the magnetic circuit.

$$\mathcal{R} = \frac{l}{\mu A} \quad (2)$$

Where $l, \mu \; and \; A$, are the length of the magnetic path, the permeability of the material and the cross-sectional area of the flux path, respectively.

$$\mu = \mu_0 \mu_r \quad (3)$$

But the permeability of the magnetic material is not constant but depends on the B-H curve; therefore, the reluctance expressed in terms of the flux density and magnetic field intensity is:

$$\mathcal{R} = \frac{Hl}{BA} \quad (4)$$

Where $H \; and \; B$, are the magnetic field intensity and flux density respectively.

From Ampere's law, the magnetomotive force (MMF is calculated as:

$$F = NI = \sum Hl \quad (5)$$

The phase windings, however, consist of two coils placed on diametrically opposite poles; thus, the total MMF is:

$$F = 2NI \quad (6)$$

Since the flux lines in a circuit complete their path through the yokes and poles of the stator and rotor, and the air gap, the total MMF is expressed as:

$$2NI = 2\left(H_{sy}l_{sy} + H_{sp}l_{sp} + H_g l_g + H_{ry}l_{ry} + H_{rp}l_{rp}\right) \quad (7)$$

Where $H_{sy}, H_{sp}, H_g, H_{ry}, H_{rp}$, are the magnetic field intensities of the stator yoke, stator pole, air gap, rotor yoke and rotor pole, respectively, and $l_{sy}, l_{sp}, l_g, l_{ry}, l_{rp}$, are the lengths of the stator yoke, stator pole, airgap, rotor yoke and rotor pole, respectively.

Because the path of the air gap is complex and thus determining its length is difficult, the MMF due to the air gap is represented as:

$$H_g l_g = \Phi_g \mathcal{R}_g \quad (8)$$

Where Φ_g, is the flux through the air gap.

Figure 2 shows the magnetic equivalent circuit at the aligned position.

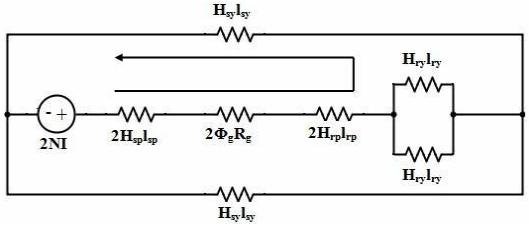

Figure 2: Magnetic equivalent circuit at the aligned position.

From equation (4), the reluctance of the yokes of the stator and rotor are calculated, and substituting equation (8) into (4), that of the air gap is calculated.

The inductance in the aligned position as a function of phase current is thus expressed as:

$$L_a(i) = \frac{4NN}{2\mathcal{R}_{sp}+2\mathcal{R}_g+2\mathcal{R}_{rp}+\mathcal{R}_{ry}+\mathcal{R}_{sy}} \quad (9)$$

Calculation of Inductance at unaligned position.

Figure 3 shows the magnetic equivalent circuit at the unaligned position.

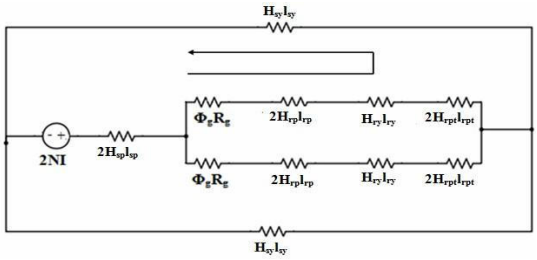

Figure 3: Magnetic equivalent circuit at the unaligned position

The MMF round the equivalent circuit is computed as:

$$2NI = 2H_{sp}l_{sp} + \Phi_g \mathcal{R}_g + 2H_{rp}l_{rp} + H_{ry}l_{ry} + 2H_{rpt}l_{rpt} + H_{sy}l_{sy} \quad (10)$$

Where H_{rpt}, l_{rpt}, are the magnetic field intensity at the rotor pole tip and the length of the rotor pole tip, respectively.

In the unaligned position, the reluctance of the air gap is considered in sections, with the total air gap reluctance represented as:

$$\mathcal{R}_g = \frac{1}{\left(\frac{1}{\mathcal{R}_1}+\frac{1}{\mathcal{R}_2}+\frac{1}{\mathcal{R}_3}\right)} \quad (11)$$

The calculation of the air gap takes into account the geometric dimensions of the various sections.

The inductance at the unaligned position is thus calculated as:

$$L_u = \frac{4NN}{2\mathcal{R}_{sp}+2\mathcal{R}_g+2\mathcal{R}_{rp}+\mathcal{R}_{ry}+2\mathcal{R}_{rpt}+\mathcal{R}_{sy}} \quad (12)$$

Using the equations above and the motor parameters, the motor's performance is simulated and evaluated with Ansys-Maxwell software.

III. Results

TABLE I: Specifications of 8/6 switched reluctance motor for investigating the effect of inductance and rotor position on motor performance.

S/No	Parameter	Value	Unit
1	Power output	15 (20)	Kw (Hp)
2	Peak current	32.61	A
3	Laminations	Steel 1010	
4	Configuration	8/6	
5	Outer core diameter	310	Mm
6	Air gap length	0.5	Mm
7	Stack length	320	Mm
8	Shaft diameter	42	Mm

9	Rotor pole arc	24	Degrees
10	Stator pole arc	22	Degrees
11	Number of stator poles	8	
12	Number of rotor poles	6	

Figure 4 shows the inductance profile versus rotor position.

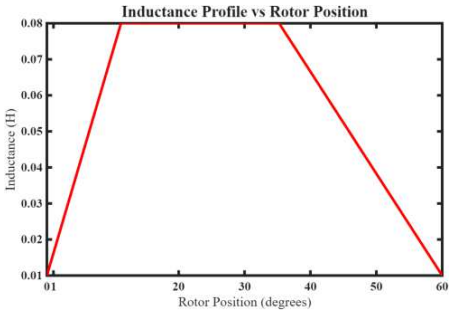

Figure 4: Inductance profile Vs rotor positions

Figure 4 represents the inductance profile for one phase over 0° to 60°. It shows maxima at aligned positions (0°, 60°) and minima at unaligned positions (30°). The steep slope of the inductance curve indicates high torque capability, as torque is proportional to the rate of change of inductance with respect to rotor position $\frac{dL}{d\theta}$.

Figure 5 shows the flux linkage distribution.

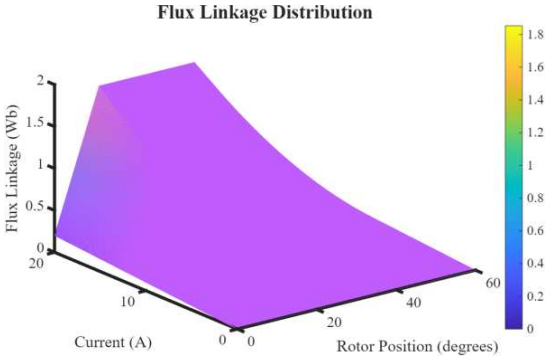

Figure 5: Flux linkage distribution

Figure 5 shows a 3D surface plot of ψ(θ, i), which is the flux linkage function of rotor position and current. This demonstrates non-linear behaviour caused by saturation at high currents, making it very important for control design and energy efficiency analysis.

Figure 6 shows the electromagnetic torque versus rotor position.

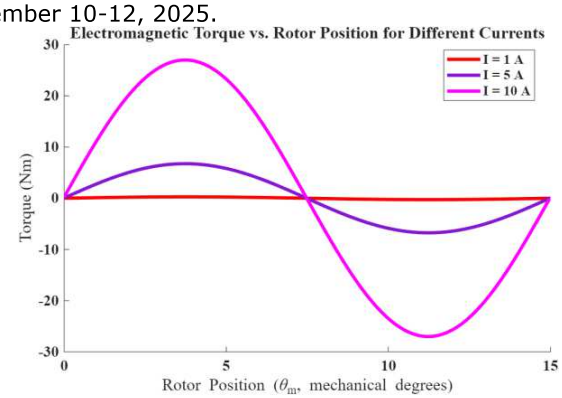

Figure 6: Electromagnetic Torque Vs rotor position at different currents

Figure 6 shows the torque at a selected current, reaching its maximum where $\frac{dL}{d\theta}$ is greatest. This plot indicates the torque generation ability, which is a key parameter for motor optimisation studies.

Figure 7 shows the flux linkage versus stator current.

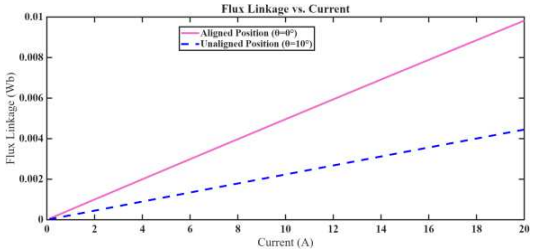

Figure 7: Flux linkage Vs current

Figure 7 depict the plot of flux linkage and the current. According to the Linear model the inductance is the sinusoidal function of rotor position, it has its maximum at 0° and 60° (aligned) and the minimum at 30° (unaligned). The saturated model is at a current of 10 A, the inductance is reduced in the neighborhood of aligned positions (0° and 60°) because of the magnetic saturation. The unaligned positions (30°) are not influenced by the effect.

Figure 8 shows the inductance versus rotor position.

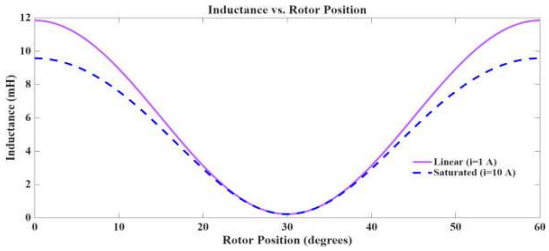

Figure 8: Inductance Vs rotor position

Figure 8 shows the plot of inductance and rotor position. When the position is aligned, the flux linkage increases proportionally at low currents; however, it saturates at high currents due to the core material's inability to support the changes. At the unaligned position, the flux linkage remains linear throughout the current because of the low magnetic flux density (no saturation).

Therefore, a high magnitude current in the aligned position reduces inductance and causes nonlinear flux linkage, which limits torque production due to the saturation effect. This suggests that excessive current in the aligned position should be avoided, leading to optimised torque and efficiency. The unaligned position still does not experience saturation effects.

Switched reluctance output models

The stator-rotor model of 8/6 SRM is shown in Figure 9.

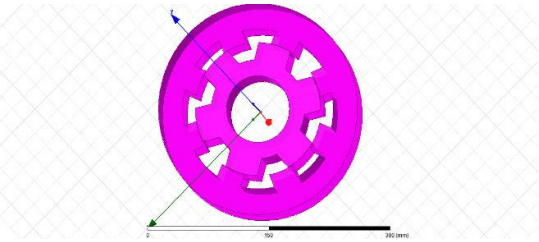

Figure 9: Stator-rotor model of 8/6 SRM

Figure 10 shows the 8/6 SRM with stator windings

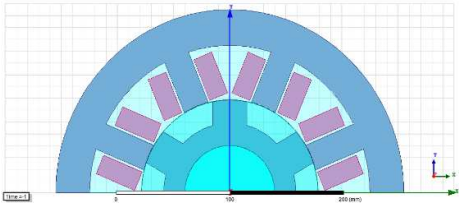

Figure 10: 8/6 SRM with windings

The mesh analysis of 8/6 SRM is shown in Figure 11.

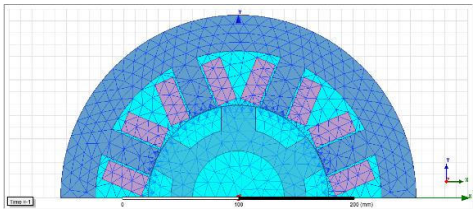

Figure 11: Mesh analysis of 8/6 SRM

TABLE II: Key performance metrics influenced by inductance and rotor position

Performance Metric	Key Findings	Implications
Inductance	- Maximum at aligned positions (0°, 60°), reduced by saturation at high currents (e.g., 10 A) - Minimum at unaligned positions (30°), no saturation effects	The variation in inductance drives torque production. Saturation at high currents can limit performance, necessitating careful control strategies.
Electromagnetic Torque	Maximum at positions where $\frac{dL}{d\theta}$ is largest, typically between aligned and unaligned positions	Indicates the motor's torque production capability, critical for design and control optimization in applications like electric vehicles.
Efficiency	Optimized by controlling current to avoid saturation at aligned positions, minimising nonlinear flux linkage and limited torque production	Proper current management is essential for maintaining high efficiency, reducing energy losses, and enhancing overall motor performance.

IV. Discussion

The results provide a comprehensive analysis of the electromagnetic properties of a motor, focusing on inductance, flux linkage, and torque in relation to rotor position and current.

Figure 4 presents the inductance profile across a rotor position range of 0° to 60°, showing that inductance reaches its maximum at aligned positions (0°, 60°) and decreases to a minimum at unaligned positions (30°). The variation in inductance is essential for torque production, as torque is directly proportional to the rate of change of inductance $\frac{dL}{d\theta}$. A steeper inductance slope signifies an increased torque capability, which is essential for optimising motor performance.

Figures 5 and 7 examine the characteristics of flux linkage, with Figure 5 showing a 3D surface plot of flux linkage (ψ) in relation to rotor position (θ) and current (i). This plot indicates nonlinear behaviour attributed to magnetic saturation at high currents. Figure 7 compares linear and saturated models, indicating that in the linear model, inductance exhibits a sinusoidal pattern with maxima at aligned positions (0° and 60°) and a minimum at the unaligned position (30°). At elevated currents (e.g., 10 A), the saturated model demonstrates a decrease in inductance at aligned positions as a result of magnetic saturation, whereas unaligned positions show no significant change. The saturation effect limits torque production.

Figures 6 and 8 illustrate the relationship between torque and inductance as functions of rotor position and current. Figure 6 shows that torque reaches its maximum at points where the rate of change of inductance $\frac{dL}{d\theta}$ is highest, highlighting the significance of this parameter for motor optimisation. Figure 8 illustrates the effect of saturation, indicating that at aligned positions, flux linkage is directly proportional to current at low levels, but exhibits nonlinearity at high currents due to limitations of the core material. In

contrast, unaligned positions exhibit linear flux linkage across all currents as a result of low magnetic flux density.

V. Conclusion

The investigation into the motor's electromagnetic characteristics provides essential insights into the relationships among inductance, flux linkage, and torque in relation to rotor position and current. The inductance profile exhibits notable variation, reaching a maximum at aligned stator positions and a minimum at unaligned positions, which directly affects torque production via its rate of change. This highlights the significance of accurate rotor position estimation in optimising torque generation capacity. The flux linkage analysis reveals the nonlinear effects of magnetic saturation at elevated currents, especially in aligned positions, resulting in reduced inductance and impeded torque output. Conversely, unaligned positions exhibit linear behaviour, remaining unaffected by saturation.

The capability for torque generation, optimised at the point where the inductance slope is steepest, represents a critical parameter in motor optimisation studies.These results have significant implications for motor design and control strategies.

References

[1] D. Xiao, S. R. Filho, G. Fang, J. Ye, and A. Emadi, "Position-Sensorless Control of Switched Reluctance Motor Drives: A Re view," IEEE Transactions on Transportation Electrification, vol. 8, no. 1, pp. 1209–1227, 2022, doi: 10.1109/TTE.2021.3110867.

[2] B. B. Sandesh, S. Kumawat, J. Pitchaimani, and K. V Gangadharan, "Design and performance analysis of a switched reluctance motor using finite element analysis and magnetic equivalent circuit model," Def Sci J, vol. 73, no. 1, p. 39, 2023.

[3] Y. Zhang, L. Chen, Z. Wang, and E. Hou, "Speed control of switched reluctance motor based on regulation region of switching angle," Energies (Basel), vol. 15, no. 16, p. 5782, 2022.

[4] R. Martua, A. R. Emir, M. Suhendra, D. Yesayevtta, A. Rizqiawan, and J. Furqani, "Control strategy comparison of the 8/6 switched reluctance motor in several inverter topologies," International Journal of Power Electronics and Drive Systems (IJPEDS), vol. 16, no. 1, pp. 117–128, 2025.

[5] R. Krishnan, Switched Reluctance Motor Drives: Modeling, Simulation, Analysis, Design, And Applications. Crc Press, 2017.

[6] H. Li, "Operational Principles and Modeling of Switched Reluctance Machines," Switched Reluctance Motor Drives, 2019, [Online]. Available: https://api.semanticscholar.org/CorpusID:199018829.

[7] J. Kim and J.-S. Lai, "Quad Sampling Incremental Inductance Measurement Through Current Loop for Switched Reluctance Motor," IEEE Trans Instrum Meas, vol. 69, no. 7, pp. 4251–4257, 2020, doi: 10.1109/TIM.2019.2949319.

[8] S. Das and G. Narayanan, "Analytical Prediction of the Unsaturated Inductance Profile of a Switched Reluctance Machine Using a Flux-Tube-Based Method," 2024 IEEE International Conference on Power Electronics, Drives and Energy Systems (PEDES), pp. 1–6, 2024, [Online].Available: https://api.semanticscholar.org/CorpusID:277980943.

[9] R. Jayapragash and C. Chellamuthu, "Development of analytical models for switched reluctance machine and their validation," Journal of Electrical Engineering and Technology, vol. 10, no. 3, pp. 990–1001, 2015.

[10] K. Diao, X. Sun, G. Bramerdorfer, Y. Cai, G. Lei, and L. Chen, "Design optimization of switched reluctance machines for performance and reliability enhance-ments: A review," Renewable and Sustainable Energy Reviews, 2022, [Online]. Available: https://api.-semanticscholar.org/CorpusID:251422062